Jurnal Teknologi

Full Paper

# DISTRIBUTION OF MAXIMUM PRINCIPAL STRESS UNDER DISTRIBUTED LOAD FROM LOADING PLATE IN SPECIMEN FOR BRAZILIAN TEST

Takashi Tsutsumi[a*], Seita Kukino[a], Rini Asnida Abdullah[b], Mohd For Mohd Amin[b]

[a]Advanced Civil Engineering Course, National Institute of Technology, Kagoshima College, Kirishima, Kagoshima, 8995193, Japan
[b]Department of Geotechnics and Transportation, Faculty of Civil Engineering, Universiti Teknologi Malaysia, 81310 UTM Johor Bahru, Johor, Malaysia

**Article history**
Received
18 *January* 2016
Received in revised form
8 *March* 2016
Accepted
18 March 2016

*Corresponding author
tsutsumi@kagoshima-ct.ac.jp

**Graphical abstract**

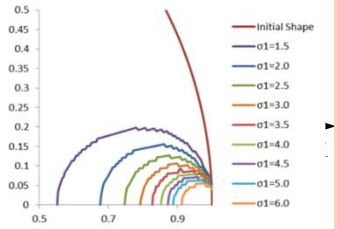


## Abstract

In this study, the distribution of the maximum principal stress in the specimen is shown under Brazilian test. Generally, Brazilian test is dealt under a pair of concentrated force to obtain the tensile strength. However, it is assumed that the contact area induces between specimen and loading plate. Therefore, the cosine curve is adopted as the distribution of load applied on the loading plates in a theoretical model for Brazilian test. The results from this study are shown in the graphical representation and compared with those under the uniform loading.

*Keywords*: Brazilian test; maximum principal stress; contact area

## Abstrak

Dalam kajian ini, pengagihan tekanan utama maksimum sampel dijalankan di bawah ujikaji Brazilian. Secara umumnya, ujikaji Brazilian adalah berkaitan sepasang beban tumpu yang dikenakan bagi memperolehi nilai kekuatan tegangan. Walaubagaimanapun, dianggapkan bahawa keluasan sentuhan wujud di antara sampel dan plat beban. Oleh itu, lengkungan kosain diadaptasi bagi membuktikan pengagihan beban yang dikenakan pada plat di dalam model teori ujikaji *Brazilian*. Keputusan dari kajian ini ditunjukkan dalam bentuk grafik dan perbandingan dibuat di antara beban seragam.

*Kata kunci*: Ujikaji Brazilian; tegasan utama maksimum; keluasan sentuhan



## 1.0 INTRODUCTION

Brazilian test is a simple and relatively inexpensive test to measure the tensile strength of a brittle material. The test is performed by placing a disk between two (rigid) plates and applying a diametrical compressive load. The test induces a biaxial stress state in which the stress at the center of the circular plane is compressive in the $x$-direction ($\sigma_x$), and tensile in the $y$-direction ($\sigma_y$). Theoretically, for an isotropic material, the tensile stress reaches a maximum at a constant magnitude of $P/(\pi a)$, where $P$ represents the applied load and $a$ represents the radius of the circular plane [1]. Because tensile strength is smaller than compressive strength for many rock materials, the material undergoes tensile failure first.

Analytical models using finite element modelling were used to evaluate the tensile stress for Brazilian test by Lemmon and Blackketter [2]. The contact area between the specimens and two loading plates was

set to 2, 4 and 8 % of the circumference of the specimen, and a uniform load was applied to the specimen. The numerical results of this study agreed well with those from a theoretical model using complex stress functions under the same conditions [3]. According to these results, the tensile stress generated near the loading plates is influenced by the contact area between the loading plates and the specimen in Brazilian test. For isotropic materials (i.e., with material properties that are uniform along each axis), the maximum tensile stress is generated at the center of disk when the contact area increases. For orthotropic materials (i.e., with material properties that differ along each of three mutually orthogonal twofold axes), the maximum tensile stress is also generated at the center of circular plane when the angle of the principal material direction to the loading direction is close to $\pi/4$. The maximum value is almost constant regardless of the contact area. On the other hand, the tensile stress is highest near the loading plate when the angle between the principal material direction and the loading direction is small, and decreases as the contact area increases. In the latter case, the contact area has a significant influence on tensile strength measurements.

In these studies, the distribution of stresses applied on the loading plate was assumed to be uniform. In reality, the maximum applied stress is generated at the center of loading plate, and decreases as the distance from the center increases. At last, the applied load seems to disappear at the edges of the loading plates.

In this study, in order to satisfy this boundary condition on the loading plate, the cosine curve is adopted as the distribution of load applied on loading plates in a theoretical model for Brazilian test. Specimens are isotropic also homogeneous and comprise a continuum without layers or micro-cracks. The elastic solution using boundary conditions shown in this study is used to obtain the distributions of the maximum principal stress in the isotropic circular specimen. Using this theoretical solution, distributions of maximum principal stress in isotropic specimen are shown.

## 2.0 FORMULATION PROBLEM

The application of opposing loads $P$ to the diametrical axis of an orthotropic disk specimen of radius $a$ is shown in Figure 1.

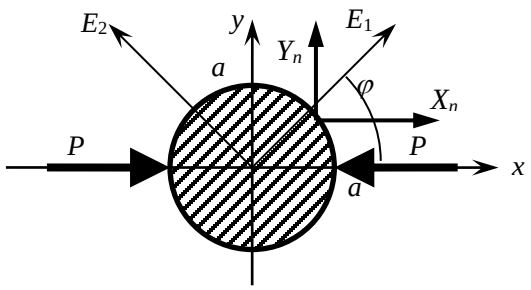


**Figure 1** Orthotropic circular plane under diametrical compression

Here, $\varphi$ represents the angle between the principal material direction and the loading direction, and $E_1$ and $E_2$ represent the respective moduli of deformation in the principal material directions. $X_n$ and $Y_n$ represent the resultant forces on a circular boundary. To approximate this condition, it is assumed that a load of magnitude $P$ is applied with the loading plate, with a width of $\omega/2$ (rad). The center of loading plate is on the $x$-axis and is where the maximum applied load is generated. The load decreases with distance from the center of the loading plate, and disappears at the edge of the loading plate as shown in Figure 2.

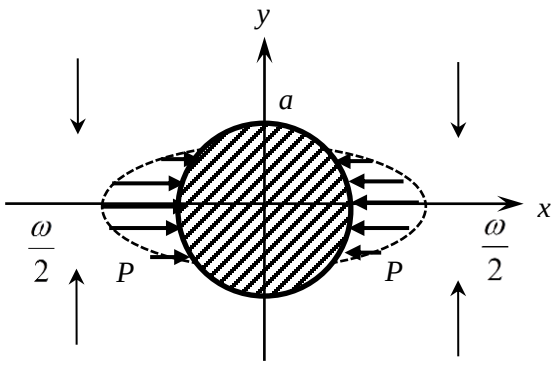


**Figure 2** Schematic diagram in this study

Boundary conditions for resultant forces are expanded into Fourier expansion with $M$ terms as shown below.

$$\left.\begin{aligned}\int_0^s X_n ds &= \beta_0 + \sum_{m=1}^{M}\left(\beta_m e^{im\theta} + \overline{\beta}_m e^{-im\theta}\right),\\ -\int_0^s Y_n ds &= \alpha_0 + \sum_{m=1}^{M}\left(\alpha_m e^{im\theta} + \overline{\alpha}_m e^{-im\theta}\right).\end{aligned}\right\} \quad (1)$$

Here, the bar denotes the complex conjugate. In this case, Fourier coefficients for resultant forces $\alpha_m$ and $\beta_m$ are given as follows.

$$\alpha_m = 0, \quad \beta_m = -\frac{i}{2}\left(b_{1n} + b_{2n} + b_{3n}\right). \quad (2)$$

$$
\left.\begin{aligned}
b_{1n} &= \frac{1}{\pi}\frac{2n\omega^2}{4\pi^2-n^2\omega^2}\cos\frac{n\omega}{4},\\
b_{2n} &= \frac{2}{\pi n}\left\{1-(-1)^n\right\}\cos\frac{n\omega}{4},\\
b_{3n} &= \frac{(-1)^n}{\pi}\times\left[-\frac{C_1\omega}{2\pi+n\omega}\left\{S_1-\cos\left(\frac{2\pi^2}{\omega}-\frac{n\omega}{4}\right)\right\}\right.\\
&\quad+\frac{C_1\omega}{2\pi-n\omega}\left\{S_1-\cos\left(\frac{2\pi^2}{\omega}+\frac{n\omega}{4}\right)\right\}\\
&\quad+\frac{S_1\omega}{2\pi+n\omega}\left\{C_1-\sin\left(\frac{2\pi^2}{\omega}-\frac{n\omega}{4}\right)\right\}\\
&\quad\left.-\frac{S_1\omega}{2\pi-n\omega}\left\{S_1-\sin\left(\frac{2\pi^2}{\omega}+\frac{n\omega}{4}\right)\right\}\right].
\end{aligned}\right\} \quad (3)
$$

$$
C_1=-\cos\frac{2\pi^2}{\omega},\quad S_1=\sin\frac{2\pi^2}{\omega}. \quad (4)
$$

The complex stress functions for an orthotropic circular plane are expanded as the series expressed below [4]:

$$
\left.\begin{aligned}
\Phi_1(z_1) &= A_0+A_1z_1+\sum_{m=2}^{M}A_mP_{1m}(z_1),\\
\Phi_2(z_2) &= B_0+B_1z_2+\sum_{m=2}^{M}B_mP_{2m}(z_2).
\end{aligned}\right\} \quad (5)
$$

Where, $P_{km}$ ($k$=1, 2, $m\geq 2$) is a power series of $m$-th order [4]. Complex coefficients $A_m$ and $B_m$ ($m\geq 0$) in Equation (5) are determined with Fourier coefficients for boundary conditions $\alpha_m$ and $\beta_m$ [3]. Now, the stress components $\sigma_x$, $\sigma_y$ and $\tau_{xy}$ are given by

$$
\left.\begin{aligned}
\sigma_x &= 2\,\mathrm{Re}\left[\mu_1^{\,2}\Phi_1'(z_1)+\mu_2^{\,2}\Phi_2'(z_2)\right],\\
\sigma_y &= 2\,\mathrm{Re}\left[\Phi_1'(z_1)+\Phi_2'(z_2)\right],\\
\tau_{xy} &= -2\,\mathrm{Re}\left[\mu_1\Phi_1'(z_1)+\mu_2\Phi_2'(z_2)\right].
\end{aligned}\right\} \quad (6)
$$

Where Re represents the real part of each of complex functions in brackets. $\Phi_k'(z_k)$ means the first derivative of with respect to $z_k$, and

$$
z_k=x+\mu_k y \qquad (k=1,\,2). \quad (7)
$$

$\mu_1$ and $\mu_2$ in the above equation are obtained as complex values of the characteristic equation [4]. The relationship between maximum principal stress $\sigma_1$ and stress components in Equation (6) is shown in Figure 3.

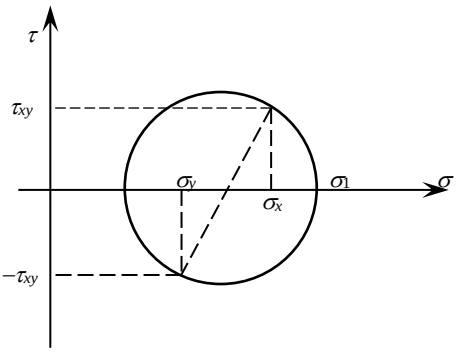


**Figure 3** Maximum principal stress in Mohr's stress circle

Therefore, the maximum principal stress $\sigma_1$ can be obtained using stress components in Equation (6) as shown in Equation (8).

$$
\sigma_1=\frac{\sigma_x+\sigma_y}{2}+\frac{\sqrt{(\sigma_x-\sigma_y)^2+4\tau_{xy}^{\,2}}}{2} \quad (8)
$$

## 3.0 RESULTS AND DISCUSSION

Figure 4 and Figure 5 show the distribution of the maximum principal stress under cosine shaped loading and uniform loading for isotropic specimen respectively. The theoretical solution used in this study was induced for orthotropic elliptic plate. In these figures, $E_2/E_1$ was set to 0.98 and the value of the major axis was set similar to the minor axis as it deals with the isotropic circular plate. In both figures, the values of maximum principal stresses were normalized by the magnitude of applied load, $P$. The contact area between loading plate and specimen is set to 4% in Figure 4 and 8% in Figure 5. The number of Fourier coefficient that is shown as $M$ in equation (1) is 45 for the loading shown in this study and 100 for uniform loading.

In Figure 4, contours mean positions of the maximum principal stress with the values of 6.0, 5.0, 4.5, 4.0, 3.5, 3.0, 2.5, 2.0 and 1.5. Values of maximum principal stress 2.5, 2.0 and 1.5 generated at the value of coordinate 0.747, 0.676 and 0.554 on loading axis in present study respectively. On the other hand, similar values of the maximum principal stress occur at the value of coordinate 0.751, 0.678 and 0.573 under uniform loading. The maximum principal stress generating on the loading radius in present study is larger than that under uniform loading. In addition, maximum principal stress spreads in the vertical direction to the loading radius in present study. The distribution shapes like pressure bulb appears in the elastic ground under concentrated force. The maximum principal stress propagates mainly in loading direction in present study. However, there are small differences between both figures.

In Figure 5, contours mean positions of maximum principal stress shows values of 3.5, 3.0, 2.5, 2.0 and 1.5. Values of maximum principal stress 2.5, 2.0 and 1.5 generated at the value of coordinate 0.764, 0.688 and 0.562 on loading axis in present study. These values are almost same as the values with the contact area of 4%. However, in this case, the value of the maximum principal stress generating around loading plate is smaller. On the other hand, similar values of the maximum principal stress generate at the value of coordinate 0.786, 0.702 and 0.573 under uniform loading. Under uniform loading, these values are smaller than those of 4% of the loading area.

Under the cosine shaped loading used in present study, the maximum deformation induces at the center of loading plate, and the value of deformation as the distance from center of loading plate increases. Finally, any deformations diminished at the edge of loading plate [5]. Therefore, the distribution of maximum principal stress in the specimen is similar to that under concentrated force [6]. Furthermore, it also explained why the value of maximum tensile stress generating on the loading axis under cosine shaped loading shown in present study is larger than that under uniform loading in orthotropic specimen [7].

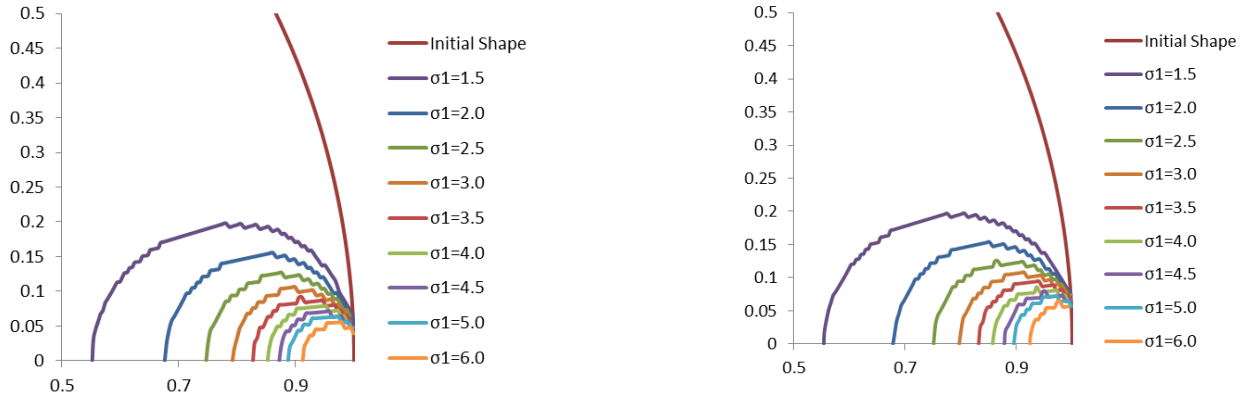


(a) Present result (b) Under uniform loading

**Figure 4** Distribution of maximum principal stress under contact area 4% in isotropic specimen

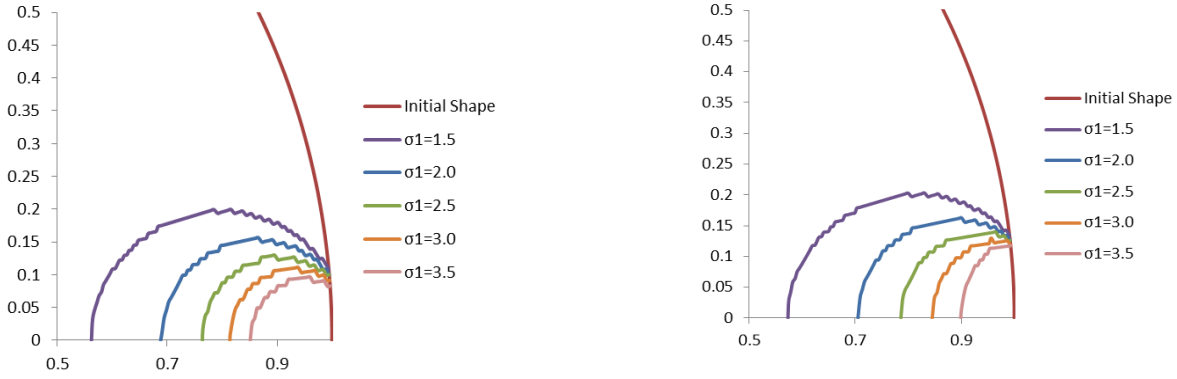


(a) Present result (b) Under uniform loading

**Figure 5** Distribution of maximum principal stress under contact area 8% in isotropic specimen

Figure 6 and Figure 7 show the distribution of the maximum principal stress under cosine shaped loading shown in present study and under uniform loading for orthotropic specimen respectively. In these figures, orthotropic ratio $E_2/E_1$ was set to 1.5 and the angle between loading direction and one of principal elastic axis $E_1$, $\varphi$ in Figure 1, was set to 0. In other words, compression was carried out in softer axis. Figure 8 and Figure 9 also show the distribution of the maximum principal stress under cosine shaped loading shown in present study and under uniform loading in orthotropic specimen. Here, the orthotropic ratio, $E_2/E_1$ was consistent as in the Figure 6 and Figure 7 but the angle between loading direction and one of principal elastic axis $E_1$ was set to $\pi/2$. In which, compression was carried out in harder axis. In Figure 6 and Figure 8, contours show positions of the maximum principal stress with the values of 6.0, 5.0, 4.5, 4.0, 3.5, 3.0, 2.5, 2.0 and 1.5. In Figure 7 and Figure 9, contours show positions of maximum principal stress with the values of 3.5, 3.0, 2.5,

2.0 and 1.5. Furthermore, contours which mean positions of maximum principal stress with values of 5.0, 4.5, 4.0 are added in Figure 9. It seems that the maximum principal stress propagates mainly in loading direction under compression in harder direction despite of distribution of loading from loading plates. On the other hand, it seems that maximum principal stress spreads in the vertical direction to the loading radius under compression in softer direction.

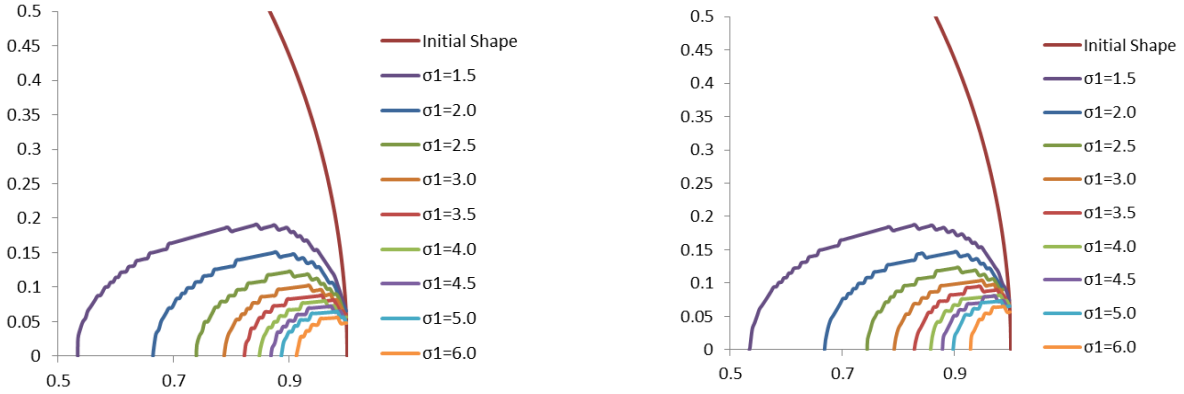


(a) Present result (b) Under uniform loading

**Figure 6** Distribution of maximum principal stress under contact area 4% for $E_2/E_1$=1.5 $\varphi$=0

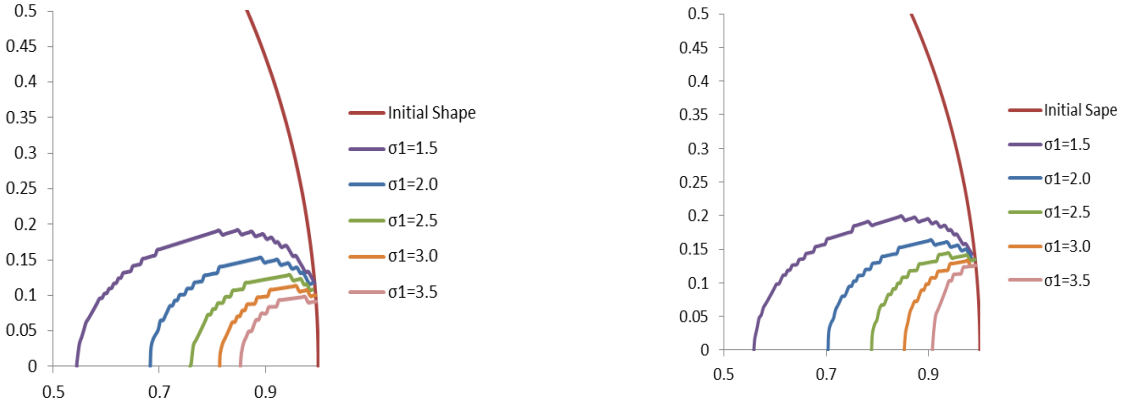


(a) Present result b) Under uniform loading

**Figure 7** Distribution of maximum principal stress under contact area 8% for $E_2/E_1$=1.5 $\varphi$=0

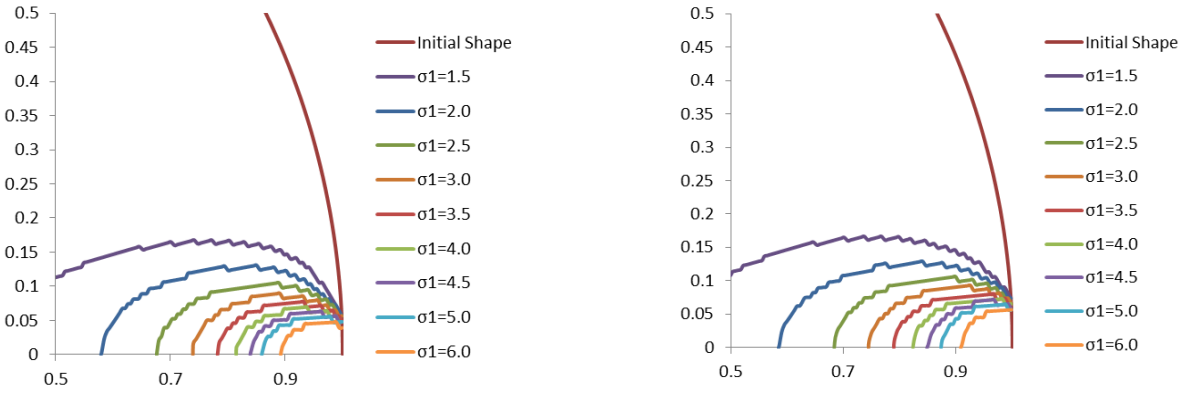


(a) Present result (b) Under uniform loading

**Figure 8** Distribution of maximum principal stress under contact area 4% for $E_2/E_1$=1.5 $\varphi$=$\pi$/2

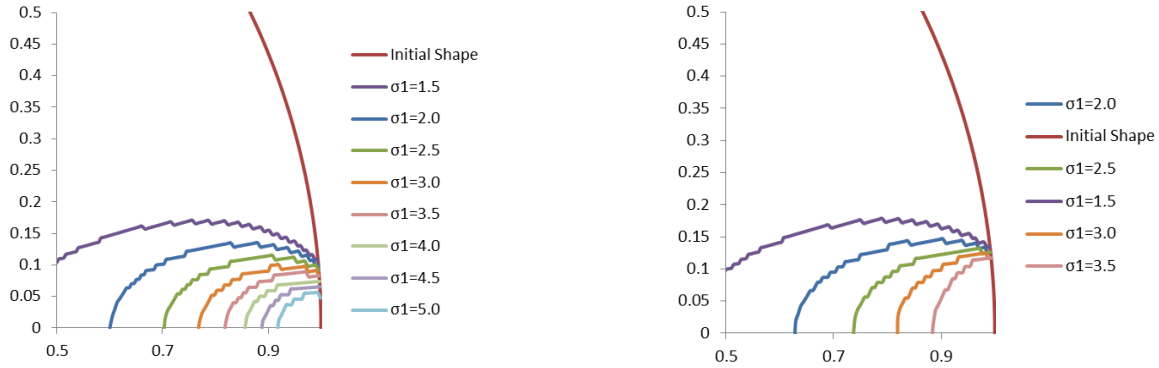


(a) Present result (b) Under uniform loading

**Figure 9** Distribution of maximum principal stress under contact area 8% for $E_2/E_1$=1.5 $\varphi=\pi/2$

## 4.0 CONCLUSION

In previous studies, concentrated forces or uniform loading were used as boundary conditions for theoretical models related to Brazilian test. To satisfy this boundary condition, the cosine curve is adopted as the distribution of applied load on the loading plate in the theoretical model for the Brazilian test. Furthermore, to obtain the distributions of maximum principal stress in the specimen, calculations were carried out using this theoretical model for selected contact areas in isotropic and orthotropic specimen. Distributions of maximum principal stress obtained from these calculations were graphically shown and compared with results obtained under uniform loading.

## References

[1] Sokolnikoff, I. S. 1956. Mathematical Theory of Elasticity. *New York, NY: McGraw-Hill.*

[2] Ulusay R. and Hudsun, J. A. 2006. The Complete ISRM Suggested Methods For Rock Characterization, *Testing and Monitoring*: 1974-2006: 181-183.

[3] Lemmon, R. K & Blackketter, D. M. 1996. Stress Analysis of an Orthotropic Material Under Diametral Compression Test. *Experimental Mechanics*. 36: 204–211.

[4] Tsutsumi, T. & Hirashima, K. 2000. Analysis of Orthotropic Circular Disks and Rings under Diametrical Loadings. *Structural Engineering and Mechanics*. 9: 37–50.

[5] Lekhnitskii, S. G. 1968. Anisotropic Plates. *New York, NY: Gordon & Breach.*

[6] Kawakubo, S., Tsutsumi, T. and Hirashima, K. 1996. Stress And Displacement Fields For An Anisotropic Elliptical Disk Subjected To Arbitrary Loads At The Boundary (in Japanese). *Transaction of JSME Series A*. 62: 1626-1633.

[7] Kukino, S. & Tsutsumi, T. 2014. Modification of Boundary Condition in Theoretical Model for Diametrical Compression Test. *Proceedings of 4th International Symposium on Technology for Sustainability*: USB Flash Drive.

[8] Jianhong, Y., Wu, F. Q. & Sun, J. Z. 2009. Estimation of the Tensile Elastic Modulus using Brazilian Disc by Applying Diametrically Opposed Concentrated Loads. *International Journal of Rock Mechanics and Mining Sciences*. 46: 568–576.

[9] Tsutsumi, T. and Kukino, S. 2015. Distribution of Tensile Stress Under Modified Boundary Condition in Theoretical Solution for the Diametrical Compression Test. *Proceedings of 13th International Congress of Rock Mechanics*: USB Flash Drive.

[10] Y. Aono, K. Tani, T. Okada and M. Sakai. 2012. The Mechanism Of Failure Near The Loading Point In The Splitting Tensile Strength Test On Tage Stone (in Japanese), *Proceedings of 41th Rock Mechanics Symposium in Japan*: 157-162.

[11] Hasaba, S., Kawamura, M. and Saito, M. 1975. Fundamental Study On The Fracture Behavior Of Convcrete Under The Splitting Loads (in Japanese), *Transaction of JSCE*. 238: 69-76.

[12] Dan, Q. D., Konietzky, H. and Herbst, M. 2013. Brazilian Tensile Strength Tests On Some Anisotropic Rocks, *International Journal of Rock Mechanics and Mining Sciences*. 58: 1–7.

[13] Chen, C. S., Pan, E. and Amadei, B. 1998. Determination Of Deformability And Tensile Strength Of Anisotropic Rock Using Brazilian Tests, *Journal of Rock Mechanics and Mining Science*. 35: 43-61.

[14] JGS2551.2002. Method For Splitting Tensile Strength Test On Rocks, *Standard of The Japanese Geotechnical Societ*: https://www. jiban. or. jp/images/JGS%202551-2002_E. pdf.

[15] Kudo, Y., Sano, O., Furukawa, K. and Nakagawa, K. 1988. Tensile Strength Distribution Of Granitic Rocks In Diametral Compression Test (in Japanese). *Transaction of JSCE*, 400, III-10: 233-241.